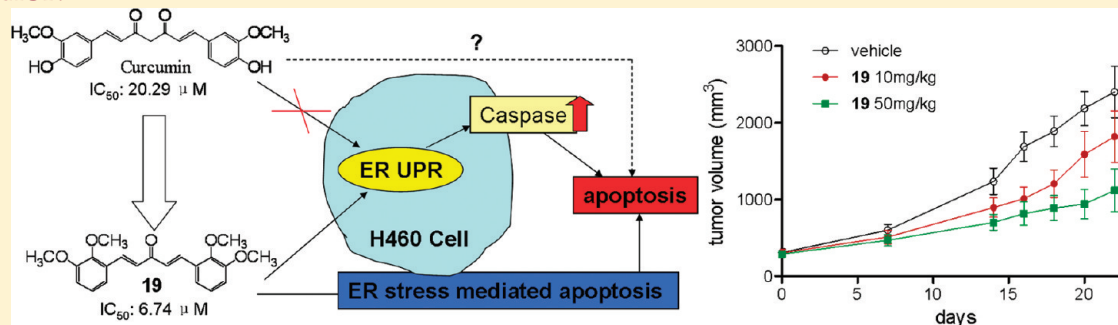


A Novel Monocarbonyl Analogue of Curcumin, (1*E*,4*E*)-1,5-Bis(2,3-dimethoxyphenyl)penta-1,4-dien-3-one, Induced Cancer Cell H460 Apoptosis via Activation of Endoplasmic Reticulum Stress Signaling PathwayYi Wang,<sup>†,‡</sup> Jian Xiao,<sup>†,‡</sup> Huiping Zhou,<sup>§</sup> Shulin Yang,<sup>†</sup> Xiaoping Wu,<sup>†</sup> Chengxi Jiang,<sup>†</sup> Yunjie Zhao,<sup>†</sup> Donglou Liang,<sup>†</sup> Xiaokun Li,<sup>†,||</sup> and Guang Liang<sup>\*,†</sup><sup>†</sup>Bioorganic and Medicinal Chemistry Research Center, School of Pharmaceutical Science, Wenzhou Medical College, Wenzhou 325035, P. R. China<sup>‡</sup>Institute of Bioengineering, Nanjing University of Science and Technology, Nanjing 210094, P. R. China<sup>§</sup>Department of Microbiology and Immunology, School of Medicine, Virginia Commonwealth University, Richmond, Virginia 23298, United States<sup>||</sup>Norman Bethune College of Medical Science, Jilin University, Changchun 130012, P. R. China

S Supporting Information

## ABSTRACT:



Endoplasmic reticulum (ER) stress-induced cancer cell apoptosis has become a novel signaling target for development of cancer therapeutic drugs. Curcumin exhibits growth-suppressive activity against a variety of cancer cells. We previously synthesized a series of monocarbonyl analogues of curcumin with strong cytotoxicity against tumor cells. In this study, we found that only compound **19** [(1*E*,4*E*)-1,5-bis(2,3-dimethoxyphenyl)penta-1,4-dien-3-one] can induce C/EBP-homologous protein (CHOP) expression in human lung cancer H460 cells. Treatment with **19** induced H460 cell apoptosis in a dose-responsive manner, and this effect was associated with corresponding increases in a series of key components in ER stress-mediated apoptosis pathway, followed by caspase cleavage and activation. However, curcumin at the same concentrations does not display such properties. CHOP knockdown by specific siRNA attenuated **19**-induced cell apoptosis, further indicating that the apoptotic pathway is ER stress-dependent. In vivo, **19** showed a dramatic 53.5% reduction in H460 xenograft tumor size after 22 days of treatment. Taken together, these mechanistic insights on the novel compound **19**, with nontoxicity, may provide us with a novel anticancer candidate.

## 1. INTRODUCTION

Endoplasmic reticulum (ER) is well-known to regulate protein synthesis, protein folding, cellular responses to stress, and intracellular calcium levels. Disturbance of ER homeostasis results in the activation of the unfolded protein response.<sup>1</sup> Accumulation of misfolded proteins in ER can cause ER stress and ultimately lead to apoptosis.<sup>2</sup> Several conditions, including nutrient deprivation, oxidative stress, changes in calcium homeostasis, failure in post-translational modifications or transport of proteins, and treatment with a variety of agents, can induce ER stress and trigger the unfolded protein response.<sup>3,4</sup> ER stress is implicated in the

pathophysiology of cancer, and ER stress-induced cancer cell apoptosis becomes a novel signaling target for development of cancer therapeutic drugs.<sup>5,6</sup> The inductions of cancer cell apoptosis by some anticancer agents such as paclitaxel,<sup>7</sup> farnesol,<sup>8</sup> and polyphyllin D<sup>9</sup> have been reported to be mediated by ER stress.

Curcumin [1,7-bis(4-hydroxy-3-methoxyphenyl)-1,6-heptadiene-3,5-dione] is a yellow compound isolated from the rhizome of the herb *Curcuma longa* L. During the past 2 decades,

Received: January 7, 2011

Published: April 19, 2011

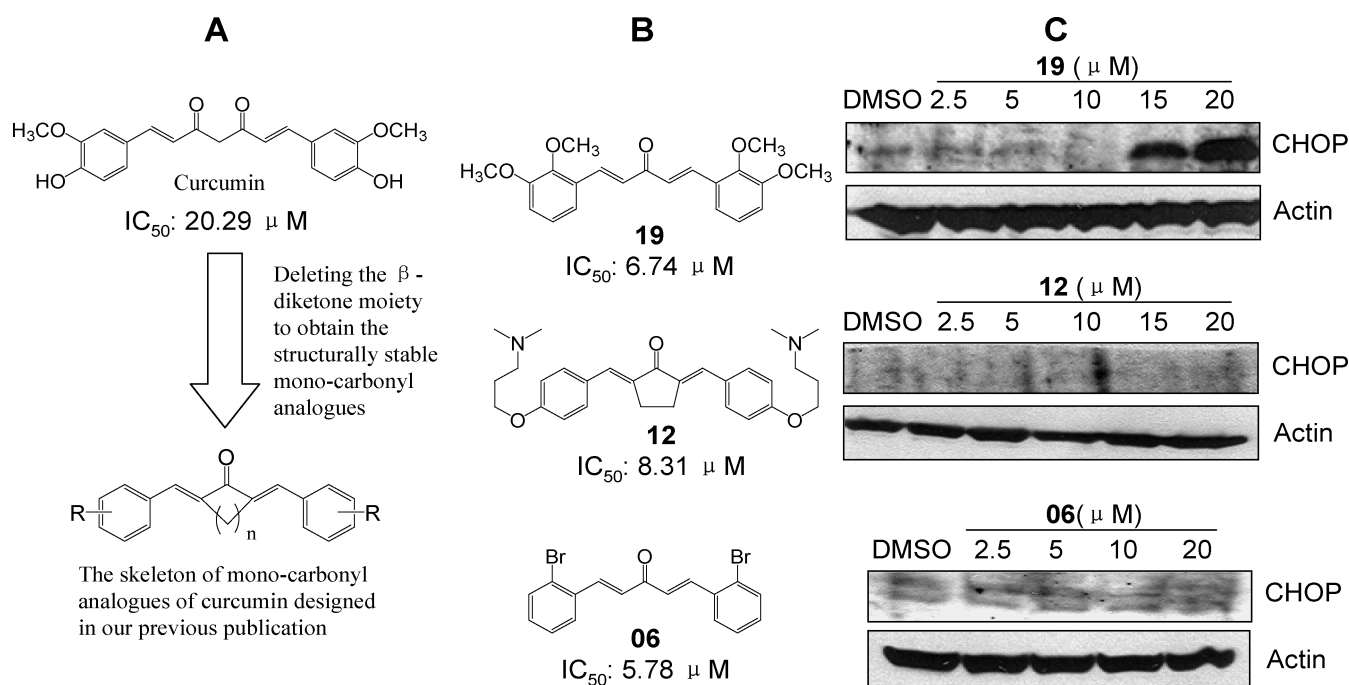


**Figure 1.** Chemical structures of compounds **06**, **12**, and **19** and their inducing CHOP expression: (A) design and skeleton of structurally stable monocarbonyl analogues of curcumin; (B) chemical structures of **06**, **12**, and **19** and their  $IC_{50}$  values against H460 cells; (C) effects of **06**, **12**, and **19** on CHOP expression. H460 cells were treated with compounds at the indicated concentrations for 24 h. Cells were collected and the total lysates isolated and examined by Western blot analysis using an anti-CHOP specific antibody. Actin is shown as a control for equal loading.

numerous studies have shown that curcumin possesses multi-functional pharmacological properties including the ability to induce apoptosis in a variety of tumor cells.<sup>10,11</sup> Recent studies suggested that curcumin-induced apoptosis may be mediated by ER stress in several cancer cell types. Pae and his co-workers<sup>12</sup> showed that curcumin-induced apoptosis of HL-60 cells is associated with its modulation of ER stress-related proteins after a 6 h treatment with curcumin at 20  $\mu$ M. A study by Scott et al.<sup>13</sup> also indicated that curcumin up-regulated C/EBP-homologous protein (CHOP) mRNA expression in colon cancer HCT-116 cells. Most recently, two independent groups demonstrated that curcumin triggers ER stress and the activation of specific cell death pathways in mouse melanoma cells<sup>14</sup> and human lung carcinoma A-549 cells,<sup>15</sup> respectively.

However, the clinical application of curcumin has been significantly limited by its instability in vitro and poor metabolic property in vivo.<sup>16</sup> Considering that the  $\beta$ -diketone moiety of curcumin may result in its instability and poor metabolic property, we previously designed a series of monocarbonyl analogues of curcumin with enhanced stability by deleting this moiety.<sup>17</sup> Our studies also demonstrated that these synthetic analogues not only enhanced stability in vitro but also significantly improved pharmacokinetic profiles in vivo.<sup>17</sup> Subsequently, a MTT assay for these compounds against seven different tumor cell lines was carried out, and three novel compounds, **06** [(1*E*,4*E*)-1,5-bis(2-bromophenyl)penta-1,4-dien-3-one], **12** [(2*E*,5*E*)-2,5-bis(4-(3-(dimethylamino)propoxy)benzylidene)cyclopentanone], and **19** [(1*E*,4*E*)-1,5-bis(2,3-dimethoxyphenyl)penta-1,4-dien-3-one] were discovered as the most efficient compounds against tumor cells.<sup>17</sup>

A recent study showed that curcumin induces apoptosis in human non-small-cell lung cancer H460 cells through ER stress and mitochondria-dependent pathways.<sup>18,19</sup> In this study, we investigated whether the induction of apoptosis by curcumin

analogues is mediated by ER stress in human NSCLC cell line H460. We provide in vitro biochemical analysis of signaling pathway modulation and assess effects on cell proliferation. Gene down-regulation by siRNA method and H460 xenograft were also used to assess the molecular mechanism and in vivo anticancer effect of compound **19**, respectively.

## 2. RESULTS

**2.1. Screening on Affecting CHOP Expression Showed That Only Compound 19 Could Activate ER Stress among Three Active Compounds in H460 Cells.** According to our previous publication,<sup>17</sup> three active compounds **06**, **12**, and **19** that exhibited good cytotoxicity against seven human cancer cell lines were chosen for this study. Their  $IC_{50}$  values, as well as that of curcumin, against H460 cells were determined using a MTT assay and are listed in Figure 1A and Figure 1B. Curcumin showed an antiproliferation effect against H460 cells with  $IC_{50}$  = 20.29  $\mu$ M, while **06**, **19**, and **12** demonstrated stronger cytotoxicity than curcumin and their  $IC_{50}$  values reached 5.78, 6.74, and 8.31  $\mu$ M, respectively. CHOP has been sufficiently proved to trigger an ER stress-specific cascade for implementation of apoptosis.<sup>20,21</sup> Therefore, the effects of these three compounds on CHOP expression were first evaluated by the Western blot method in H460 cells. As shown in Figure 1C, among these compounds, only compound **19** is able to stimulate CHOP expression after 24 h of treatment, especially at 15 and 20  $\mu$ M, suggesting that **19**, unlike other analogues, induces H460 cell apoptosis possibly via an interesting mechanism involving ER stress-apoptosis pathways.

**2.2. Compound 19 but Not Curcumin Causes ER Stress in H460 Cells.** Glucose-regulate protein/immunoglobulin heavy chain binding protein (GRP78) is reported as the gatekeeper to

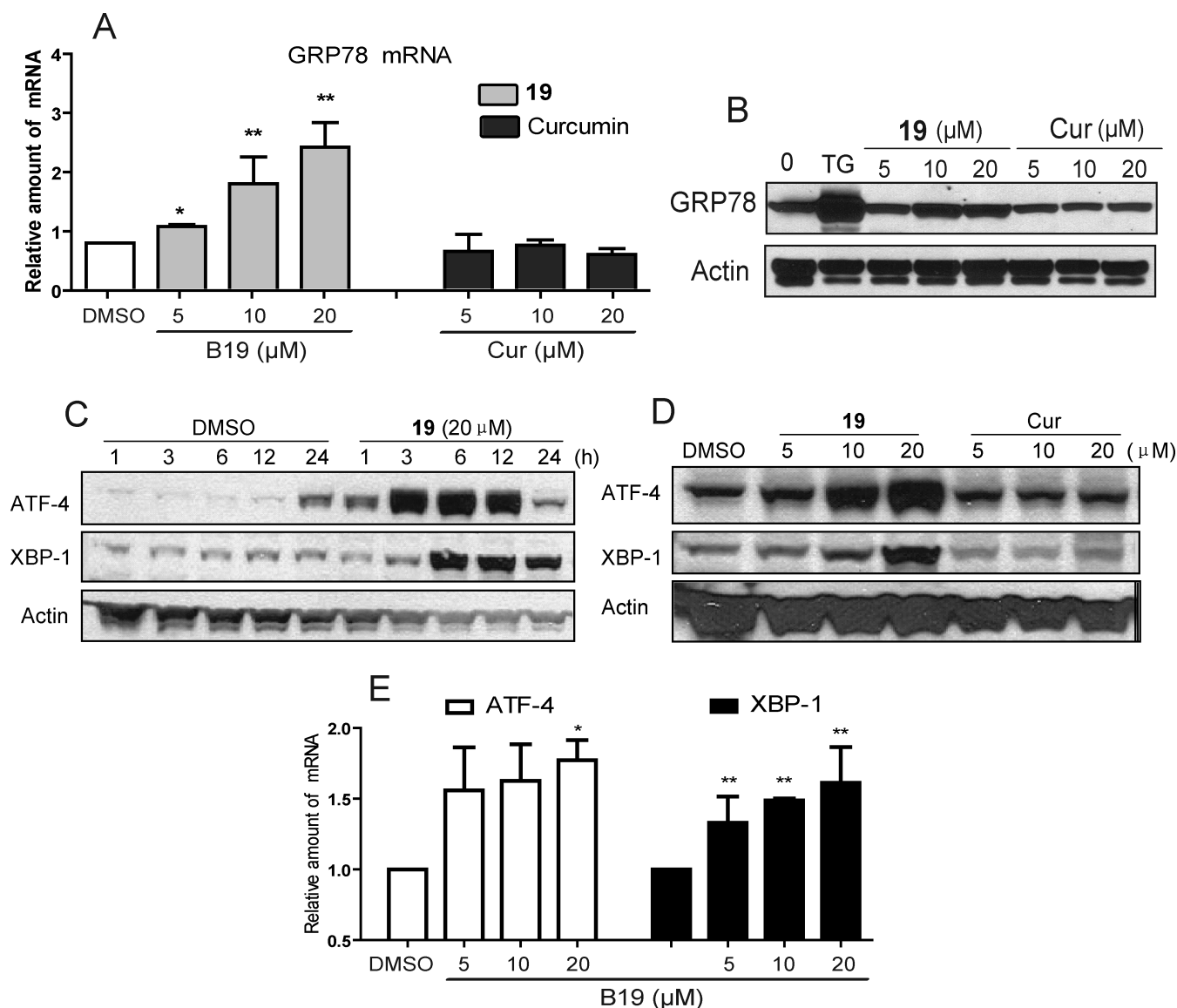


**Figure 2.** Compound 19 induces GRP78, ATF-4, and XBP-1 expression. (A) H460 cells were treated with compounds at the indicated concentrations for 1 h. GRP78 mRNA was examined by RT-qPCR. (B) Cells were treated with 19 and curcumin for 3 h, and GRP78 was examined by Western blot. (C) H460 cells were incubated with vehicle and 19 at 20  $\mu\text{M}$  for the indicated times. The protein levels of ATF-4 and XBP-1 were examined by Western blot. (D) H460 cells were treated with 19 at the indicated concentrations for 6 h. The ATF-4 and XBP-1 expressions were detected by Western blot. (E) H460 cells were harvested after incubation with 19 at the indicated concentrations for 3 h. ATF-4 and XBP-1 mRNA were examined by RT-qPCR. All RT-qPCR results were calculated and represented as the percent of vehicle control, and actin was always shown as a control for equal loading in RT-qPCR and Western blotting experiments ((\*)  $p < 0.05$ , (\*\*)  $p < 0.02$ , significantly different from vehicle group).

the activation of the ER stress.<sup>22</sup> We thus measured both mRNA and protein expression of GRP78 after 19 or curcumin treatment. As shown in Figure 2A and 2B, both mRNA expression and protein expression of GRP78 were increased 3 h after 19 treatment, while no significant increase could be observed in the curcumin-treated group. In addition, RT-qPCR analysis revealed that GRP78 mRNA increased in a dose-dependent manner at 3 h after the cells were incubated with 19. Following the gatekeeper, we tested the expressions of the downstream activating transcription factor 4 (ATF-4) and X-box binding proteins 1 (XBP-1) in 19- or curcumin-treated H460 cells using both Western blot and RT-PCR. The time course result indicated that 20  $\mu\text{M}$  compound 19 treatment for 6 h resulted in the protein levels of ATF-4 and XBP-1 reaching the peak (Figure 2C).

Western blot analysis revealed that increases in protein expression levels of both ATF-4 and XBP-1 were detected in a dose-dependent manner at 6 h after the cells were incubated with 19 (Figure 2D), while no significant increase could be seen in the 20  $\mu\text{M}$  curcumin-treated cells. These results were further supported by Figure 2E illustrating that 19 induces the up-regulation of both ATF-4 and XBP-1 mRNAs dose-dependently.

CHOP induction is probably the most sensitive to ER stress response, and CHOP is considered as a marker of commitment of ER stress-induced apoptosis.<sup>21</sup> During ER stress, all three arms of the unfolded protein response (UPR) including ATF-4 and XBP-1 pathways induce transcription of CHOP gene.<sup>23</sup> We have already found that 19 was able to induce CHOP expression in the previous section. Here, we further demonstrated the ability of 19

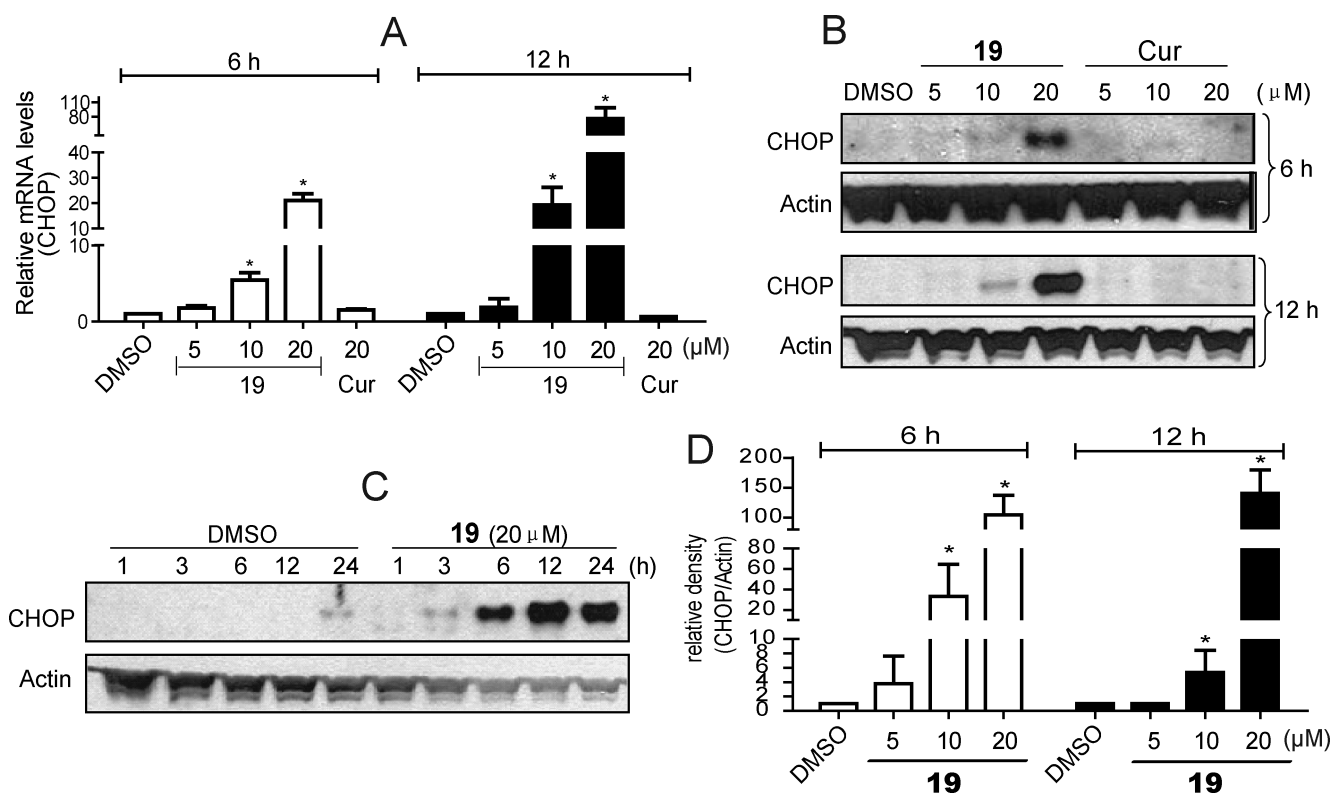


**Figure 3.** Compound **19** induces CHOP expression. H460 cells were collected after incubation with compounds at the indicated concentrations for the indicated times. (A) CHOP mRNA was examined by RT-PCR. (B, C) CHOP examined by Western blot. Actin is shown as a control for equal loading. (D) Western blot results from (C) was calculated and represented as the percent of control ((\*)  $p < 0.02$ , significantly different from vehicle group).

and curcumin to increase CHOP at both protein and mRNA levels. As shown in Figure 3A, exposing H460 cells to **19** for both 6 and 12 h noticeably increased CHOP mRNA expression in a dose-dependent manner, while curcumin at 20  $\mu\text{M}$  has no effect on CHOP mRNA level. Western blotting analysis further showed that CHOP protein expression was apparently increased 6–24 h after **19** treatment and reached the peak at 12 h (Figure 3B). Figure 3C and Figure 3D showed that compound **19** induced CHOP protein up-regulation in a dose-dependent manner. Similarly, CHOP expression was not detectable in curcumin-treated cells.

In addition, in the commitment phase of ER stress-induced apoptosis, inositol requiring 1 (IRE1) triggers apoptosis by recruiting and activating c-jun N-terminal kinase (JNK), which directly phosphorylates the downstream c-Jun and induce p-53 expression in the cell apoptosis pathway.<sup>23</sup> We therefore examined the effects of **19** on c-Jun phosphorylation and p53 expression using the Western blot method. As shown in Figure 4A, c-Jun was found to begin to be phosphorylated at 3 h of **19** treatment (20  $\mu\text{M}$ ). The phosphorylation increased with time and peaked at 12 h after **19** treatment. In Figure 4B, **19** at 20  $\mu\text{M}$  apparently activated the c-Jun phosphorylation, while curcumin at the same concentration showed no effect on it. Besides c-Jun phosphorylation, the IRE1 pathway has been recently identified to activate caspase cascade by the downstream regulator p-53. As shown in Figure 4C and Figure 4D, **19** treatment significantly increased the expression of p-53 in both time and dose dependent manner during 1–12 h after **19** treatment. The expression of p-53 decreased after 12 h of treatment. Curcumin still showed a negative result.

All upstream signals ultimately led to caspase activation to finish the execution of ER stress-induced apoptosis.<sup>23</sup> We next examined the **19**-induced ER stress-mediated apoptotic downstream events after commitment. The Western blot in Figure 4E indicates that the cleavage of procaspase-3 was observed after treatment with **19** for 24 h. Similar results were observed for the activation of caspase-9 (Figure 4F). However, at this concentration, curcumin was not able to activate caspase 3 and 9. These results indicate that the caspase signals are involved in the ER stress-mediated apoptotic pathway induced by **19**.

**2.3. Compound 19 Induces H460 Cell Death through Apoptotic Pathway.** Compound **19** or curcumin was administrated to H460 cells in different doses (5, 10, and 20  $\mu\text{M}$ ), respectively. Cell growth was recorded by light microscope, and cell viabilities were determined by CellTiter-Glo kit assay. After **19** treatment for 24 h, the cells underwent significant morphologic changes under a microscope. As shown in Figure 5A and Figure 5B, **19** at different concentrations induces H460 cell death more potently than curcumin at the same concentrations ( $P < 0.01$ ). The cell viability assay demonstrated that **19** ranged from 2.5 to 30  $\mu\text{M}$  reduced cell survival in a dose-dependent manner (Figure 5B). The leading curcumin, however, showed relatively poor activity. At 20  $\mu\text{M}$ , about 16% of H460 cells survived after 24 h of treatment with **19**, while there was about 70% cell viability in the curcumin group. We next assessed the effects of **19** and curcumin on the induction of apoptosis in H460 cells by flow cytometry. The results in Figure 5C showed that **19** dose-dependently increased H460 apoptosis after 6 h of treatment. **19** at 20  $\mu\text{M}$  significantly induced higher H460 cell apoptosis rate (29.63%) than from curcumin treatment (12.02%). Taken



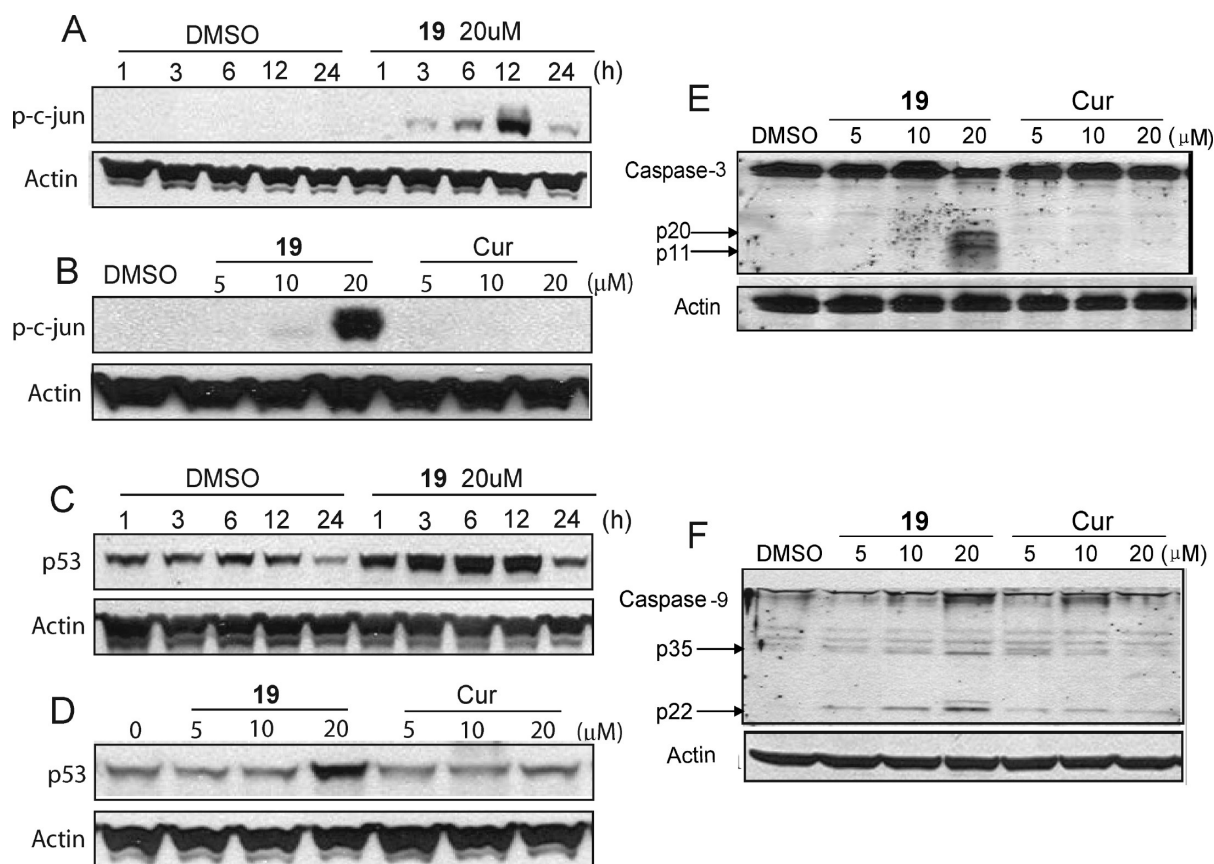


**Figure 4.** Compound 19 induces p53 expression, c-Jun phosphorylation, and procaspase cleavage. (A, C) H460 cells were incubated with compounds at 20  $\mu\text{M}$  for the indicated times. The proteins were examined by Western blot. (B, D) H460 cells were incubated with compounds at the indicated concentration for 12 h. The p53 and p-c-Jun were examined by Western blot. (E, F) H460 cells were incubated with compounds at the indicated concentrations for 24 h. The activation of caspases 3 and 9 were examined by Western blot analysis using anti-caspase-3 (p30, p17) and anti-caspase-9 (p47, p35, p22). In parts A–F, actin is shown as a control for equal loading.

together, these data indicated that 19 induced H460 cell death possibly through an apoptotic pathway involving ER stress.

**2.4. Reduction of CHOP Expression Inhibits 19-Induced H460 Cell Death.** In order to further confirm that ER stress plays an important role in the induction of H460 cell apoptosis by compound 19, we constructed the lentiviral siRNA for the *CHOP* gene, which encoded the CMV-promoted EGFP marker as an internal control. H460 cells were transfected with the vector that contained the *CHOP* siRNA. H460 cells were infected with serial dilutions of concentrated lentivirus, and the titers were determined by counting EGFP-expressing cells after 48 h using fluorescent microscopy. Figure 6A showed that more than 65% of the H460 cells were transfected with lentiviral siRNA. The reduction of *CHOP* expression was confirmed by Western blot assay. After transfected with lentiviral siRNA for *CHOP*, *CHOP* expression was significantly reduced in 19-treated cells compared to the vector-transfected control group (Figure 6B). Furthermore, to confirm that reduction of *CHOP* expression inhibits 19-induced H460 cell death, we treated *CHOP* siRNA-transfected H460 cells with 19 and curcumin. Figure 6C and Figure 6D showed that when *CHOP* expression in H460 cells is silenced, cell apoptosis induced by 19 was significantly reduced compared with the control group ( $P < 0.05$ ). Since *CHOP* is an extremely key protein in ER stress, these results indicate that 19-induced cell apoptosis is, at least partly, mediated by ER stress pathway.

**2.5. Compound 19 Suppressed Tumor Growth in Vivo.** We further investigated the in vivo antitumor efficacy of 19 using BALB/cA nude mouse. Tumor was established by subcutaneously implanting the H460 cells with  $3 \times 10^6$  (in 100  $\mu\text{L}$ ) into the mice. To establish a better administration and to exclude the pharmacokinetic and metabolic effects, a water-soluble preparation of 19 was prepared using a patented liposome technique. Once daily ip injection of 19 at doses of 10 and 50 mg/kg or vehicle was commenced when the tumor reach a volume of 100–300  $\text{mm}^3$ . As shown in Figure 7A, treatment with 19 resulted in a significant reduction in tumor volume compared to that observed in vehicle group ( $P < 0.05$ ,  $P < 0.01$ ). A dose-dependent inhibition of tumor growth by 19 at 10 and 50 mg/kg with treated versus control ( $T/C$ ) of 75.8% and 46.5% was observed on day 22 after treatment, respectively. The data showed a potent inhibitory effect of 19 on H460 tumor growth in vivo, which was possibly associated with ER-stress-mediated apoptosis in tumor cells.

### 3. DISCUSSION AND CONCLUSION

Besides mitochondria and death receptors, recent studies have suggested that the ER also participates in execution of apoptosis as a subcellular player.<sup>24,25</sup> Clinical data support the potential of drugs that inhibit the normal functions and homeostasis of the ER in treatment of malignancies like cancer. Liao et al.<sup>7</sup> reported that ER

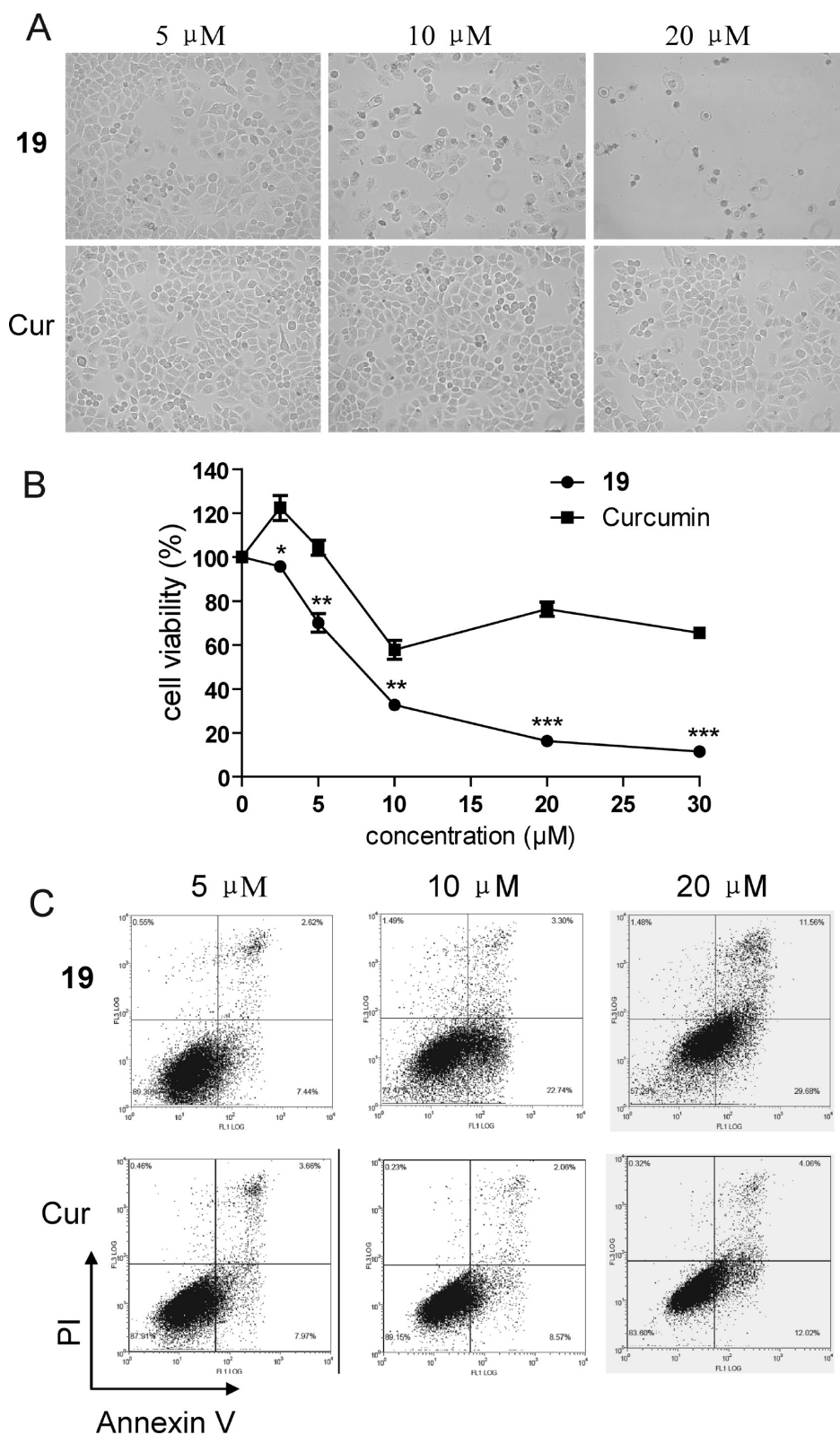


**Figure 5.** Compound 19 and curcumin induce cell death in H460 cells. (A) Cells were treated with 19 and curcumin for 24 h at the indicated concentrations. The images were obtained by microscope with 20× amplification. (B) Cell viability was carried out as described in Experimental Section, and the data were calculated as percent of the viability of vehicle-treated cells (\* $p < 0.05$ , \*\* $p < 0.02$ , \*\*\* $p < 0.01$ , significantly different from curcumin group). (C) Flow cytometric assay of H460 cells after 6 h of incubation with the indicated concentrations (5–20  $\mu\text{M}$ ) of 19 and curcumin. Cells were stained with annexin V and PI.

stress contributed to paclitaxel-induced apoptosis. Sequential ER stress has been reported to be critical in  $\alpha$ -TEA<sup>26</sup> and combined

niflumic acid–ciglitazone<sup>27</sup> treatment-induced apoptosis in human lung cancer cells. Resveratrol induces apoptosis in human NPC cells

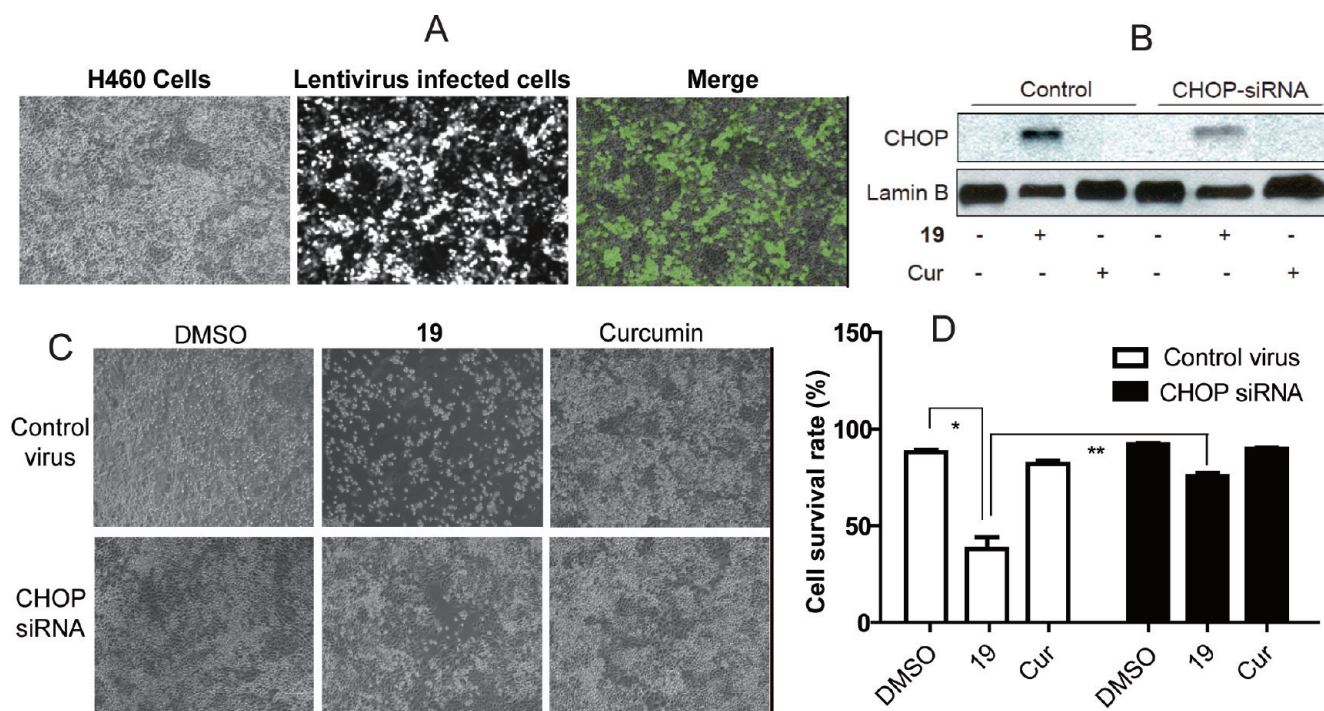


**Figure 6.** CHOP knockdown inhibits 19-induced H460 cell apoptosis. (A) H460 cells were transfected with CHOP siRNA virus using the method as described in Experimental Section. At 48 h after transfection, the CHOP- and EGFP-expressing cells were counted under a fluorescent microscope. (B) Nonspecific or CHOP siRNA was transfected into H460 cells. After 48 h, cells were treated with 19 (10  $\mu$ M) or curcumin (10  $\mu$ M) for 6 h and then CHOP expression was determined by Western blotting with actin as a control for equal loading. (C, D) Nonspecific or CHOP siRNA was transfected into H460 cells. After 48 h, cells were treated with 19 (10  $\mu$ M) or curcumin (10  $\mu$ M) for 24 h, respectively. The images were obtained by microscope with 20 $\times$  amplification (C). The cell survival experiment was carried out as described in Experimental Section, and the data were calculated as percent of the viability of nontransfected and DMSO-treated cells (D) ((\*)  $p < 0.01$ , significantly different from vehicle-treated group; (\*\*)  $p < 0.05$ , significantly different from CHOP siRNA-transfected group).

also through regulation of multiple apoptotic pathways including ER stress.<sup>28</sup> Recently, it has been suggested that manipulation of ER stress might enhance the efficacy of chemotherapeutic drugs, and the ER stress-mediated apoptotic pathways provide new anticancer targets for the development of antitumor drugs.<sup>5,6</sup>

Curcumin at more than 30  $\mu$ M exerts cytotoxicity on H460 cells through induction of apoptosis, and apoptotic cell death involves ER stress signaling pathway.<sup>19</sup> In the cytotoxic screening assay, analogues 06, 12, and 19 exhibited powerful cytotoxic effects against human lung cancer H460 cells with  $IC_{50}$  less than 10  $\mu$ M, indicating that they possess much higher activity than curcumin. In order to develop novel antitumor agents by ER stress-mediated mechanism, we tested their ability to raise the expression of CHOP, a hallmark of ER stress-mediated apoptotic pathway. Figure 1C showed that only 19 induced CHOP overexpression in H460 cells, indicating that 19 may perform its antitumor effect through a different mechanism from that of the other analogues.

This is the first report to demonstrate that the curcumin analogue has the ability to cause ER stress. Because cellular Michael adduct formation is responsible for ER stress,<sup>29</sup> it is speculated that curcumin may disrupt disulfide bond formation by the electrophilic olefin ketone on its chemical structure, consequently causing accumulation of unfolded proteins and ER stress. This concept is also supported by the observation that the curcumin derivative tetrahydrocurcumin that loses the ability to form Michael adducts did not cause ER stress.<sup>12</sup> In this study, compound 19 with a more electrophilic dienone moiety

and two electron-donating methoxyls activates ER stress at a much lower concentration compared with curcumin. In the structure of 12, the cyclization by a cyclopentanone locks the conformation of dienone and increases the stereospecific blockade, which may result in a decrease of electrophilicity of 12 dienone. In addition, the electron-withdrawing bromo substituents may contribute to a descending electrophilicity of 06 (Figure 1). These data suggest that an electrophilic dienone moiety may play an important role in the induction of ER stress by the curcumin analogues.

Then the exact molecular mechanism by which 19 causes ER stress-mediated cell apoptosis is revealed by degrees. GRP78, a member of a glucose-regulated protein family (GRPs), is reported as the gatekeeper to the activation of the ER stress.<sup>22</sup> Our data found that 19 could increase GRP78 mRNA level 1 h after treatment and protein expression 3 h after treatment. Once GRP78 activated, PKR-like ER kinase (PERK) phosphorylates eukaryotic initiation factor 2 (eIF2) and then up-regulates ATF4 expression. ATF4 is activated and moves to the nucleus and induces genes of XBP1. IRE1 seems to be the last arm of the UPR to be activated. It triggers apoptosis by recruiting and activating JNK, which directly phosphorylates the downstream c-Jun.<sup>23,30,31</sup> Subsequently, we detected the 19-induced activation of three sensor proteins, including PERK, ATF-6, and IRE1, via monitoring of their downstream molecules ATF-4, XBP-1, and p-c-Jun at 6–12 h after 19 treatment, respectively. These data intensively indicated that compound 19 might trigger the ER stress-dependent apoptotic pathway.



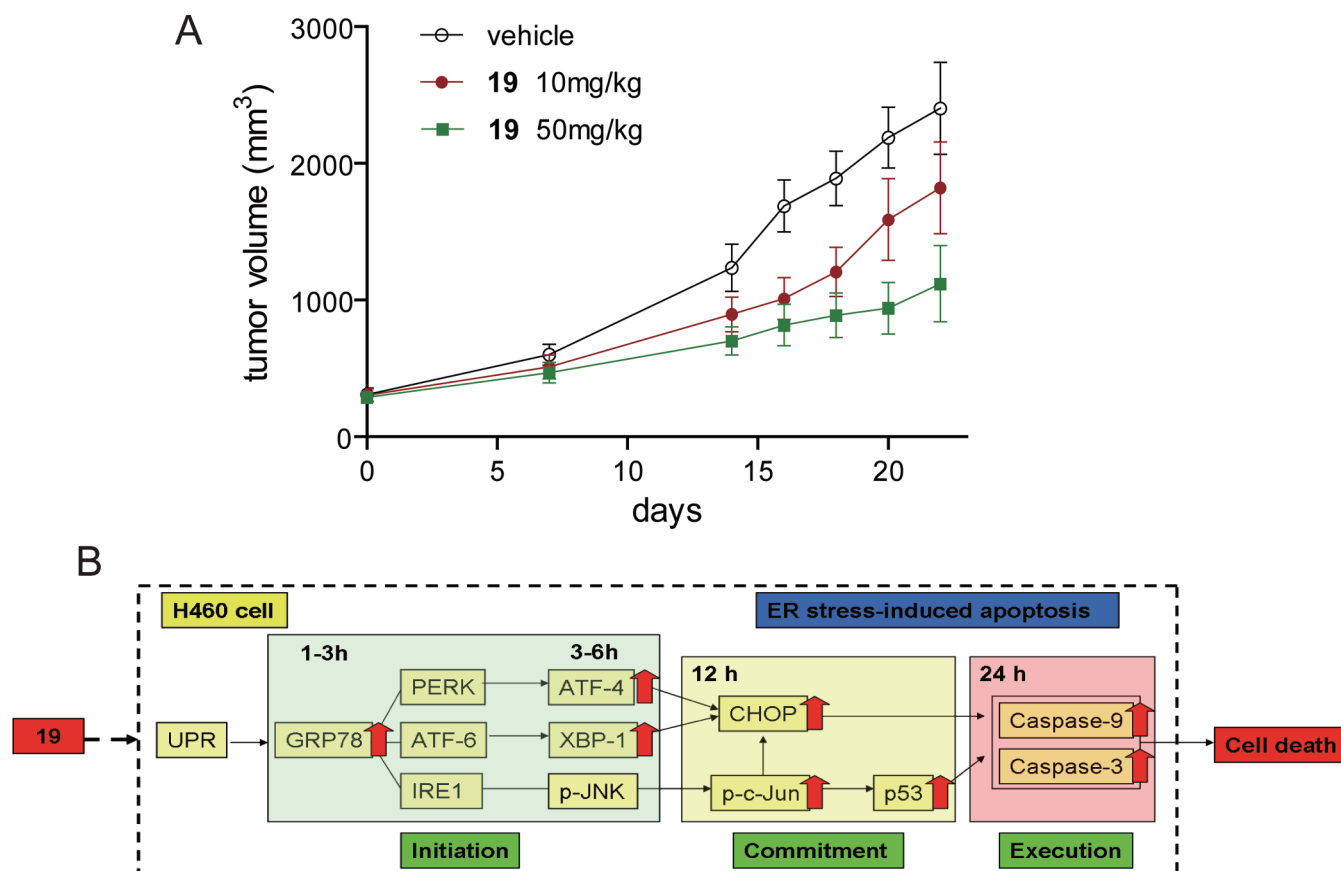


**Figure 7.** (A) Compound **19** inhibits human tumor xenograft growth in a model of human non-small-cell lung cancer model: effect of 10 mg/kg (●), 50 mg/kg (■), or vehicle (○) on growth of tumor xenografts. Xenografts were established sc in athymic mice and allowed to reach a volume of 100–300 mm<sup>3</sup> before treatment. Once daily ip injection of **19** or vehicle then commenced and was continued for the duration of the experiment. Points represent mean of seven mice, and bars represent the standard deviation (SD). (B) Proposed model of signaling pathway involved in **19**-induced apoptosis of H460 cells. Compound **19** induces the UPR response, leading to ordinal increases of downstream GRP78, ATF-4, XBP-1, CHOP, and p-c-Jun, p53 and eventual activation of caspase-3/9 to cause cell apoptosis in H460 cells.

The ATF-4 and XBP-1 activations have been reported to increase *CHOP* gene expression, triggering ER stress-specific cascade for implementation of apoptosis. The up-regulation of both *CHOP* mRNA and *CHOP* protein expression after **19** treated H460 cells for 12 h (Figure 3) indicates that the **19**-induced ER stress has developed into the commitment phase toward apoptosis. It has been reported that the phosphorylation of c-Jun could activate Bcl-2 family proteins.<sup>23,32</sup> Figure 4C and Figure 4D also illustrate that treatment of H460 cells with **19** for 6–12 h induced the enhancement of transcription factor p53. Although being thought of as main regulators in mitochondrial-mediated apoptotic pathway, several members of the Bcl-2 family of proteins are important in the ER stress downstream pathway.<sup>23,32</sup> Recently, p53 and p53-up-regulated modulator of apoptosis (PUMA) have been reported to have an important role in ER stress as downstream regulators of IRE1 signaling.<sup>33</sup> Kudoh et al.<sup>34</sup> found that a novel p53-responsive gene D4S234E is accumulated in the ER and induces apoptosis in response to DNA damage.

All upstream signals ultimately lead to caspase activation, resulting in the ordered and sequential dismantling of the cell to finish the execution of ER stress-induced apoptosis.<sup>23,31</sup> Cleavage and activation of caspases 3 and 12 have been observed in different studies on ER stress-induced human cancer cell apoptosis.<sup>23,30,31,35</sup> Two groups reported that caspase-12 can

directly trigger caspase-9 activation and apoptosis independently of the mitochondrial cytochrome *c*/Apaf-1 pathway.<sup>36,37</sup> Figure 4E and 4F demonstrated that **19** was able to induce the cleavage of caspases 3 and 9. Overall, our data demonstrated the capacity of **19** to activate all key proteins in initiation, commitment, and execution phases of ER stress. Figure 7B showed a proposed signaling model leading to development of ER stress-induced apoptosis induced by **19**.

Our data further confirmed that H460 cells are sensitive to compound **19** treatment at concentrations ranging from 5 to 30  $\mu$ M by cell viability assay and flow cytometry, while curcumin did not exhibit good activity at the indicated concentrations (Figure 5). The above data demonstrated that ER stress was involved in **19**-induced cell apoptosis. However, we do not yet know whether **19**-induced cell apoptosis is ER stress-dependent or not. Transfection of cells with *CHOP* or *GRP78* siRNA reduced ER stress-mediated human colon cancer cell apoptosis.<sup>38</sup> Knockdown of *CHOP* by specific siRNAs also attenuated desipramine-induced<sup>39</sup> and  $\gamma$ -tocotrienol-induced ER stress-mediated apoptotic cascade.<sup>40</sup> To show direct evidence for the role of ER stress in **19**-induced apoptosis, *CHOP* siRNA transfection was used to compare **19**-induced ER-stress-dependent and non-ER-stress-dependent apoptosis. The result in Figure 6 is consistent with other studies that show *CHOP* as a proapoptotic protein, and more importantly, it solidly supports



that **19**-induced apoptosis is, at least partially, ER stress-dependent. In spite of the data supporting our hypothesis, other apoptotic mechanisms may also be involved in **19**-induced apoptosis. Caspase-3 activation and p53 phosphorylation also play important roles in mitochondria-mediated apoptotic pathway.<sup>30–32</sup> In addition, the leading curcumin has been reported to exert anticancer effects by multitargeting mechanisms.<sup>10,19</sup> Therefore, although this work only focuses on the ER stress-mediated apoptosis, further studies are necessary to establish such notions.

The activation of ER stress-mediated apoptosis in cancer cells may open up the possibility to extend the therapeutic options for **19** in cancer treatment. Indeed, besides the cellular effects, we have shown that compound **19** is highly effective in inhibiting tumor growth in a H460 xenograft mouse model. At the same time, we obtained evidence that **19** exhibited high safety in a toxicity test in mice (Figures S1–S3 in Supporting Information). Taken together, novel compound **19** exhibited antitumor effects on human lung cancer H460 cells both in vitro and in vivo via an ER stress-mediated mechanism. These properties of **19** could be further explored in the development of safe and effective anticancer agents for the treatment of non-small-cell lung cancer.

## 4. EXPERIMENTAL SECTION

**4.1. Chemistry.** Curcumin was purchased from Sigma Chemical Co. (St. Louis, MO). Curcumin analogues **06**, **12**, and **19** were synthesized by direct aldol condensation of substituted benzaldehyde with acetone or cyclopentanone in alkaline media and were structurally identified by using MS and <sup>1</sup>H NMR analysis, as described in our previous paper.<sup>17</sup> Before use in biological experiments, compounds were recrystallized from CHCl<sub>3</sub>/EtOH and HPLC was used to determine their purity (**19**, 99.67%; **06**, 99.01%; **12**, 99.49%). Their structures are shown in Figure 1A and Figure 1B.

**4.2. Cell Lines and Reagents.** Human lung carcinoma cell line H460 was purchased from ATCC (Manassas, VA). The tumor cells are cultured in RPMI 1640 medium (Invitrogen, Carlsbad, CA) supplemented with 5% heat-inactivated FBS (Atlanta Biologicals Inc., Lawrenceville, GA) and 100 U/mL penicillin and streptomycin (Mediatech Inc., Manassas, VA) and incubated at 37 °C with 10% CO<sub>2</sub>. ApoAlert annexin V kit was purchased from Clotech Bio Company (Mountain View, CA). CellTiter-Glo kit was from Promega Corporation (Madison, WI). Antibodies including anti-CHOP, anti-XBP-1, anti-ATF-4, anti-caspase-3 p30/17, anti-caspase-9 p35, anti-p53, anti-p-c-Jun, anti-GRP78/Bip, anti-actin, anti-lamin B, goat anti-mouse IgG-HRP, goat anti-rabbit IgG-HRP, donkey anti-goat IgG-HRP, and anti-IGM were purchased from Santa Cruz Biotechnology (Santa Cruz, CA). Ambion RNAqueous kit was purchased from Applied Biosystems Inc. (Foster City, CA).

**4.3. MTT (Methyl Thiazolyl Tetrazolium) Assay.** All experiments were carried out 24 h after cells were seeded. Tested compounds were dissolved in DMSO and diluted with 1640 medium to final concentrations of 100, 33.3, 11.1, and 3.7 μg/mL. The tumor cells were incubated with test compounds for 72 h before the MTT assay. A fresh solution of MTT (5 mg/mL) prepared in NaCl solution (0.9%) was added to each single well of the 96-well plate. The plate was then incubated in a CO<sub>2</sub> incubator for 3 h. Cells were dissolved with 100 μL of DMSO and then analyzed in a multiwell-plate reader at 570 nm. Curcumin was applied as positive control.

**4.4. Cell Viability Assay.** H460 cells (5 × 10<sup>3</sup> cells/well) were seeded in 96-well plates overnight. Culture medium was replaced with fresh medium containing various concentrations of compound **19** or curcumin. Compounds were dissolved in DMSO and directly added to

culture medium (final concentration, 5, 10, and 20 μM) and incubated for 24 h. Cell viability was observed by microscope and evaluated using the CellTiter-Glo kit (Promega Corporation, Madison, WI) following the manufacturer's protocol at different time points. Absorbance was measured at 450 nm using the 1420 multilabel counter (PerkinElmer, Waltham, MA).

**4.5. Flow Cytometric Analysis.** H460 cells were placed in a 6 mm plate for 6 h and then treated with varying doses (5, 10, and 20 μM) of **19** and curcumin for 24 h. Cells were washed by PBS 3 times, then digested by 0.25% pancreatin–EDTA. After centrifugation, cells were resuspended in 0.5 mL of PBS. Cells were then stained with annexin V and propidium iodide (PI) in the presence of 100 mg/mL RNase and 0.1% Triton X-100 for 30 min at 37 °C. Flow cytometric analysis was performed using a fluorescence-activated cell sorter (Beckman Coulter, Inc., Fullerton, CA).

**4.6. Western Blot Analysis.** After treatment, H460 cells were washed and harvested with PBS. Cell lysis was carried out at 0 °C by vigorous shaking for 10 min in lysis buffer containing 50 mmol/L Tris-HCl (pH 7.4), 150 mmol/L NaCl, 1% NP40, and 0.1% SDS, supplemented with protease and phosphatase inhibitor cocktails I and II (Sigma, St. Louis, MO). The protein concentration was determined. After addition of sample loading buffer, protein samples were electrophoresed and then transferred to nitrocellulose membranes (Bio-Rad, Hercules, CA). The blots were blocked for 1 h at room temperature with fresh 5% nonfat milk in TBS and then incubated with specific primary antibody in TBS with 5% nonfat milk. Following three washes with TBS, the blots were incubated with horseradish peroxidase-conjugated secondary antibodies. The transferred proteins were incubated with Western Lightning chemiluminescence reagent for 1 min followed by visualization with X-ray film. The density of the immunoreactive bands was analyzed using Image J computer software (NIH).

**4.7. RNA Isolation and Real-Time Quantitative PCR.** Total mRNA was isolated from cells using Ambion RNAqueous kit after treatment with compounds or control DMSO. The high-capacity cDNA archive kit was used to obtain first-strand cDNAs of mRNAs. The mRNA levels of CHOP, XBP-1, ATF4, and GRP78 are quantified by specific gene expression assay kits and primers on iQ5 Multicolor real-time PCR detection system (Bio-Rad, Hercules, CA) and normalized to internal control β-actin mRNA. PCR primer sequences were as follows: CHOP, sense, 5'-CTGAATCTGCACCAAGCATGA-3', antisense, 5'-AAGGTGGGTAGTGTGGCCC-3'; XBP-1, sense, 5'-GCGCCTCACGCACCTG-3', antisense, 5'-GCTGCTACTCTGTTTTTCAGTTTCC-3'; ATF-4, sense 5'-TGGCTGGCTGTGGATGG-3', antisense, 5'-TCCCGGAGAAGGCATCCT-3'; GRP78, sense 5'-TCCTGCGTCGGCGTGT-3', antisense, 5'-GTTGCCCTGATCGTTGGC-3'; actin, sense 5'-CCTGGCACCAGCACAAT-3', antisense, 5'-GCCGATCACACGGAGTACT-3'.

**4.8. Construction of Lentiviral siRNA for CHOP.** The sense sequence of the siRNA cassettes specifically targeting the nucleotides of CHOP was designed through siRNA target finder (Ambion, Austin, TX). A two-step polymerase chain reaction (PCR) strategy was performed using two separate reverse primers to generate a siRNA expression cassette (SEC) consisting of human U6 promoter and a hairpin siRNA cassette plus terminator and subcloned into pGL3.7 vector, which encodes the CMV-promoted EGFP (enhanced green fluorescent protein) marker as internal control. The resulting lentiviral siRNA vector was confirmed by restriction enzyme digestion and DNA sequencing. The sequence of CHOP siRNA is 5'-GCAGGAAATC-GAGCGCCTGAC-3'. The recombinant lentiviruses were produced by transient transfection of H460 cells using FuGene 6 Transfection reagent (Roche Inc., Nutley, NJ). Briefly, H460 cells were cultured in high glucose DMEM, supplemented with 10% fetal bovine serum (FBS), penicillin/streptomycin (100 U/mL), and 500 μg/mL of G418. The

subconfluent cells in a 10 cm culture dish were co-transfected with lentiviral vector (10  $\mu\text{g}$ ) and the lentiviral packaging vectors pRSV-REV (2  $\mu\text{g}$ ), pMDLg/pRRE (5  $\mu\text{g}$ ), and the vesicular stomatitis virus G glycoprotein (VSVG) expression vector pMD2G (3  $\mu\text{g}$ ). The viruses were collected from the culture supernatants on days 2 and 3 after transfection, concentrated by ultracentrifugation for 1.5 h at 25 000 rpm, and resuspended in PBS. Titers were determined by infecting H460 cells with serial dilutions of concentrated lentivirus and counting EGFP-expressing cells after 48 h under a fluorescent microscope.

**4.9. In Vivo Antitumor Study.** All animal experiments complied with the Wenzhou Medical College Policy on the Care and Use of Laboratory Animals. Five-week-old to 6-week-old athymic BALB/cA nu/nu female mice (18–24 g) were purchased from Animal Center of China Pharmaceutical University (Nanjing, China). Animals were housed at a constant room temperature with a 12 h:12 h light/dark cycle and fed a standard rodent diet and water. H460 cells were harvested and injected subcutaneously into the right flank ( $3 \times 10^6$  cells in 100  $\mu\text{L}$  of PBS) of 7-week-old female BALB/cA nude mice. When tumors reach a volume of 100–300  $\text{mm}^3$  on all mice on day 10, treated mice were intraperitoneally (ip) injected with a water-soluble preparation of compound **19** in PBS at a dosage of 10 or 50 mg/kg, whereas control mice were injected with liposome vehicle in PBS. The tumor volumes were determined by measuring length ( $l$ ) and width ( $w$ ) and calculating volume ( $V = lw^2/2$ ) as described elsewhere.<sup>41</sup>

**4.10. Statistical Methods.** Student's  $t$  test was employed to analyze the differences between sets of data. Statistics were performed using GraphPad Pro (GraphPad, San Diego, CA). A  $p < 0.05$  was considered significant.

## ■ ASSOCIATED CONTENT

**S Supporting Information.** Results from safety assessment of **19** in vivo. This material is available free of charge via the Internet at <http://pubs.acs.org>.

## ■ AUTHOR INFORMATION

### Corresponding Author

\*Phone: (+86)-577-86699892. Fax: (+86)-577-86689983. E-mail: cui.liang1234@163.com.

### Author Contributions

<sup>†</sup>These authors contributed equally to this paper.

## ■ ACKNOWLEDGMENT

The work was supported by grants from the National Natural Science Foundation of China (Grants 20802054, 30872308, and 30901819), Young Talent Funding of Zhejiang Department of Health (Grant 2009QN020), Key Project of Wenzhou Science and Technology Bureau (Grants Y20090009 and Y20100006), and Zhejiang Natural Science Fund (Grants Y2090358, Y2090680, Y2090668, and Y4090261).

## ■ ABBREVIATIONS USED

ER, endoplasmic reticulum; UPR, unfolded protein response; CHOP/GADD153, C/EBP-homologous protein/growth arrest and DNA damage-inducible gene 153; GRP78, glucose-regulate protein 78; ATF-4, activating transcription factor 4; XBP-1, X-box binding proteins 1

## ■ REFERENCES

- (1) Schröder, M.; Kaufman, R. J. The mammalian unfolded protein response. *Annu. Rev. Biochem.* **2005**, *74* (1), 739–789.
- (2) Breckenridge, D.; Germain, M.; Mathai, J.; Nguyen, M.; Shore, G. Regulation of apoptosis by endoplasmic reticulum pathways. *Oncogene* **2003**, *22* (53), 8608–8618.
- (3) Li, G.; Scull, C.; Ozcan, L.; Tabas, I. NADPH oxidase links endoplasmic reticulum stress, oxidative stress, and PKR activation to induce apoptosis. *J. Cell Biol.* **2010**, *191* (6), 1113–1125.
- (4) Bussche, A.; Machida, R.; Li, K.; Loevinsohn, G.; Khander, A.; Wang, J.; Wakita, T.; Wands, J.; Li, J. Hepatitis C virus NS2 protein triggers endoplasmic reticulum stress and suppresses its own viral replication. *J. Hepatol.* **2010**, *53* (5), 797–804.
- (5) Armstrong, J.; Flockhart, R.; Veal, G.; Lovat, P.; Redfern, C. Regulation of endoplasmic reticulum stress-induced cell death by ATF4 in neuroectodermal tumor cells. *J. Biol. Chem.* **2010**, *285* (9), 6091–6100.
- (6) Hill, D. S.; Martin, S.; Armstrong, J. L.; Flockhart, R.; Tonison, J. J.; Simpson, D. G. Combining the endoplasmic reticulum stress-inducing agents bortezomib and fenretinide as a novel therapeutic strategy for metastatic melanoma. *Clin. Cancer Res.* **2009**, *15* (4), 1192–1198.
- (7) Liao, P. C.; Tan, S. K.; Lieu, C. H.; Jung, H. K. Involvement of endoplasmic reticulum in paclitaxel-induced apoptosis. *J. Cell. Biochem.* **2008**, *104* (4), 1509–1523.
- (8) Joo, J. H.; Liao, G.; Collins, J. B.; Grissom, S. F.; Jetten, A. M. Farnesol-induced apoptosis in human lung carcinoma cells is coupled to the endoplasmic reticulum stress response. *Cancer Res.* **2007**, *67* (16), 7929–7936.
- (9) Siu, F. M.; Ma, D. L.; Cheung, Y. W.; Lok, C. N.; Yan, K.; Yang, Z. Proteomic and transcriptomic study on the action of a cytotoxic saponin (polyphyllin D): induction of endoplasmic reticulum stress and mitochondria-mediated apoptotic pathways. *Proteomics* **2008**, *8* (15), 3105–3017.
- (10) Bar-Sela, G.; Epelbaum, R.; Schaffer, M. Curcumin as an anticancer agent: review of the gap between basic and clinical applications. *Curr. Med. Chem.* **2010**, *17* (3), 190–197.
- (11) Javadi, P.; Hertan, L.; Kosoff, R.; Datta, T.; Kolev, J.; Mick, R. Thioredoxin reductase-1 mediates curcumin-induced radiosensitization of squamous carcinoma cells. *Cancer Res.* **2010**, *70* (5), 1941–1950.
- (12) Pae, H. O.; Jeong, S. O.; Jeong, G. S.; Kim, K. M.; Kim, H. S.; Kim, S. A. Curcumin induces pro-apoptotic endoplasmic reticulum stress in human leukemia HL-60 cells. *Biochem. Biophys. Res. Commun.* **2007**, *353* (4), 1040–1045.
- (13) Scott, D. W.; Loo, G. Curcumin-induced GADD153 upregulation: modulation by glutathione. *J. Cell. Biochem.* **2007**, *101* (2), 307–320.
- (14) Bakhshi, J.; Weinstein, L.; Poksay, K. S.; Nishinaga, B.; Bredesen, D. E.; Rao, R. V. Coupling endoplasmic reticulum stress to the cell death program in mouse melanoma cells: effect of curcumin. *Apoptosis* **2008**, *13* (7), 904–914.
- (15) Lin, S. S.; Huang, H. P.; Yang, J. S.; Wu, J. Y.; Hsia, T. C.; Lin, C. C. DNA damage and endoplasmic reticulum stress mediated curcumin-induced cell cycle arrest and apoptosis in human lung carcinoma A-549 cells through the activation caspases cascade and mitochondrial-dependent pathway. *Cancer Lett.* **2008**, *272* (1), 77–90.
- (16) Anand, P.; Kunnumakkar, A. B.; Newman, R. A.; Aggarwal, B. B. Bioavailability of curcumin: problems and promises. *Mol. Pharmaceutics* **2007**, *4* (6), 807–818.
- (17) Liang, G.; Shao, L. L.; Wang, Y.; Zhao, C. G.; Chu, Y. H.; Xiao, J.; Zhao, Y.; Li, X.; Yang, S. Exploration and synthesis of curcumin analogues with improved structural stability both in vitro and in vivo as cytotoxic agents. *Bioorg. Med. Chem.* **2009**, *17* (6), 2623–2631.
- (18) Dempke, W. C.; Suto, T.; Reck, M. Targeted therapies for non-small cell lung cancer. *Lung Cancer* **2010**, *67* (3), 257–274.
- (19) Wu, S. H.; Hang, L. W.; Yang, J. S.; Chen, H. Y.; Lin, H. Y.; Chiang, J. H.; Lu, C. C.; Yang, J. L.; Lai, T. Y.; Ko, Y. C.; Chung, J. G.

Curcumin induces apoptosis in human non-small cell lung cancer NCI-H460 cells through ER stress and caspase cascade-and mitochondria-dependent pathways. *Anticancer Res.* **2010**, *30* (6), 2125–2133.

(20) Tsukano, H.; Gotoh, T.; Endo, M.; Miyata, K.; Tazume, H.; Kadomatsu, T.; Yano, M.; Iwawaki, T.; Kohno, K.; Araki, K.; Mizuta, H.; Oike, Y. The endoplasmic reticulum stress-C/EBP homologous protein pathway-mediated apoptosis in macrophages contributes to the instability of atherosclerotic plaques. *Arterioscler., Thromb., Vasc. Biol.* **2010**, *30* (10), 1925–1932.

(21) Oyadomari, S.; Mori, M. Roles of CHOP/GADD153 in endoplasmic reticulum stress. *Cell Death Differ.* **2004**, *11*, 381–389.

(22) Bertolotti, A.; Zhang, Y.; Hendershot, L. M.; Harding, H. P.; Ron, D. Dynamic interaction of BiP and ER stress transducers in the unfolded-protein response. *Nat. Cell Biol.* **2000**, *2*, 326–332.

(23) Szegezdi, E.; Logue, S. E.; Gorman, A. M.; Samali, A. Mediators of endoplasmic reticulum stress-induced apoptosis. *EMBO Rep.* **2006**, *7* (9), 880–885.

(24) Rao, R. V.; Hermel, E.; Castro-Obregon, S.; del Rio, G.; Ellerby, L. M.; Ellerby, H. M.; Bredesen, D. E. Coupling endoplasmic reticulum stress to the cell death program. Mechanism of caspase activation. *J. Biol. Chem.* **2001**, *276* (36), 33869–33874.

(25) Oyadomari, S.; Araki, E.; Mori, M. Endoplasmic reticulum stress-mediated apoptosis in pancreatic beta-cells. *Apoptosis* **2002**, *7* (4), 335–345.

(26) Tiwary, R.; Yu, W.; Li, J.; Park, S. K.; Sanders, B. G.; Kline, K. Role of endoplasmic reticulum stress in alpha-TEA mediated TRAIL/DR5 death receptor dependent apoptosis. *PLoS One* **2010**, *5* (7), e11865.

(27) Kim, B. M.; Maeng, K.; Lee, K. H.; Hong, S. H. Combined treatment with the Cox-2 inhibitor niflumic acid and PPAR $\gamma$  ligand ciglitazone induces ER stress/caspase-8-mediated apoptosis in human lung cancer cells. *Cancer Lett.* **2011**, *300* (2), 134–144.

(28) Huang, T. T.; Lin, H. C.; Chen, C. C.; Lu, C. C.; Wei, C. F.; Wu, T. S.; Liu, F. G.; Lai, H. C. Resveratrol induces apoptosis of human nasopharyngeal carcinoma cells via activation of multiple apoptotic pathways. *J. Cell. Physiol.* **2011**, *226* (3), 720–728.

(29) Wang, X.; Thomas, B.; Sachdeva, R.; Arterburn, L.; Frye, L.; Hatcher, P. G.; Cornwell, D. G.; Ma, J. Mechanism of arylating quinone toxicity involving Michael adduct formation and induction of endoplasmic reticulum stress. *Proc. Natl. Acad. Sci. U.S.A.* **2006**, *103*, 3604–3609.

(30) Rasheva, V. I.; Domingos, P. M. Cellular responses to endoplasmic reticulum stress and apoptosis. *Apoptosis* **2009**, *14* (8), 996–1007.

(31) Schleicher, S. M.; Moretti, L.; Varki, V.; Lu, B. Progress in the unraveling of the endoplasmic reticulum stress/autophagy pathway and cancer: implications for future therapeutic approaches. *Drug Resist. Updates* **2010**, *13* (3), 79–86.

(32) Mielke, K.; Herdegen, T. JNK and p38 stresskinases—degenerative effectors of signal-transduction-cascades in the nervous system. *Prog. Neurobiol.* **2000**, *61* (1), 45–60.

(33) Kieran, D.; Woods, I.; Villunger, A.; Strasser, A.; Prehn, J. H. Deletion of the BH3-only protein puma protects motoneurons from ER stress-induced apoptosis and delays motoneuron loss in ALS mice. *Proc. Natl. Acad. Sci. U S A.* **2007**, *104* (51), 20606–20611.

(34) Kudoh, T.; Kimura, J.; Lu, Z. G.; Miki, Y.; Yoshida, K. D4S234E, a novel p53-responsive gene, induces apoptosis in response to DNA damage. *Exp. Cell Res.* **2010**, *316* (17), 2849–2858.

(35) Loughlin, D. T.; Artlett, C. M.; Kango-Singh, M. Precursor of advanced glycation end products mediates ER-stress-induced caspase-3 activation of human dermal fibroblasts through NAD (P) H oxidase 4. *PLoS One* **2010**, *5* (6), e11093.

(36) Rao, R. V.; Castro-Obregon, S.; Frankowski, H.; Schuler, M.; Stoka, V.; Del Rio, G. Coupling endoplasmic reticulum stress to the cell death program: an Apaf-1-independent intrinsic pathway. *J. Biol. Chem.* **2002**, *277*, 21836–21842.

(37) Morishima, N.; Nakanishi, K.; Takenouchi, H.; Shibata, T.; Yasuhiko, Y. An endoplasmic reticulum stress-specific caspase cascade in apoptosis. *J. Biol. Chem.* **2002**, *277*, 34287–34294.

(38) Huang, S. M.; Cheung, C. W.; Chang, C. S.; Tang, C. H.; Liu, J. F.; Lin, Y. H. Phloroglucinol derivative MCPP induces cell apoptosis in human colon cancer. *J. Cell. Biochem.* **2011**, *112* (2), 643–652.

(39) Ma, J.; Qiu, Y.; Yang, L.; Peng, L.; Xia, Z.; Hou, L. N.; Fang, C.; Qi, H.; Chen, H. Z. Desipramine induces apoptosis in rat glioma cells via endoplasmic reticulum stress-dependent CHOP pathway. *J. Neuro-Oncol.* **2010**, *101* (1), 41–48.

(40) Wali, V. B.; Bachawal, S. V.; Sylvester, P. W. Endoplasmic reticulum stress mediates gamma-tocotrienol-induced apoptosis in mammary tumor cells. *Apoptosis* **2009**, *14* (11), 1366–1377.

(41) Sun, J.; Blaskovich, M. A.; Knowles, D.; Qian, Y.; Ohkanda, J.; Bailey, R.; Hamilton, A. D.; Sebt, S. Antitumor efficacy of a novel class of non-thiol-containing peptidomimetic inhibitors of farnesyltransferase and geranylgeranyltransferase I. *Cancer Res.* **1999**, *59* (19), 4919–4926.